Control of the particle deposition in inkjet-printed droplets

E.L. Talbot[1], L. Yang[1], A. Berson[2] and C.D. Bain[1]; [1] Department of Chemistry, Durham University, Durham, DH1 3LE, United Kingdom; [2] School of Engineering and Computing Sciences, Durham University, Durham, DH1 3LE, United Kingdom

Abstract

Radial flow in drying droplets forms a ring stain deposit. By controlling the amount of radial flow using an evaporation-driven sol–gel transition in laponite suspensions, a uniform deposit can be achieved. Droplets gel from the contact line inwards, reducing particle flow to the droplet periphery. The method is demonstrated for picolitre droplets relevant to inkjet printing. Internal flows are visualized using high-speed imaging techniques. The final deposits are characterized by scanning electron microscopy and white light interferometry.

Introduction

A ring stain is a common unwanted output resulting from the drying of a sessile droplet. When the contact line of a droplet is pinned throughout drying, particles inside the droplet move radially outwards, forming a ring stain [1]. This phenomenon is referred to as the "coffee ring effect". Such deposits have been observed for many solvent systems on a wide range of substrates [2, 3, 4, 5].

We use suspensions of laponite - a nano-particulate clay - to control the radial flow within water droplets and obtain uniform deposits. The improved homogeneity in the deposit arises from a sol-gel transition during evaporation. The increased concentration of laponite due to evaporation of the solvent causes the propagation of a gelling front from the contact line inwards, reducing radial motion of the particles and thus inhibiting build up of a ring stain [6].

The internal flows and propagation of the gelling front were followed by high-speed imaging of tracer particles inside picolitre droplets. The particle distributions within dried deposits were measured for water droplets loaded with polystyrene spheres and laponite by microscopy and interferometry. The laponite and polystyrene sphere concentrations can be tuned to vary the deposit profile from a ring to a pancake or a dome.

Experimental

Laponite RD suspensions (Rockwood) were prepared in high purity water (MilliQ). Inkjet droplets were ejected from an 80-μm nozzle (Microfab, AJ-ABP-01), controlled with a Microfab driver unit (Microfab JetDrive III Controller CT-M3-02). Droplets were deposited onto glass substrates (as-received) with impact velocities of $1-2\,\mathrm{ms}^{-1}$. Droplets dried at an ambient temperature of 21 °C and a relative humidity of 50%.

Internal flows within drying droplets were visualized by high speed imaging (Photron APS-RX) on an inverted microscope (see Fig. 1). Droplets were seeded with polystyrene spheres as tracers for the fluid flow. Simultaneously, shadowgraph images of the droplet profile were acquired with a second camera (Optronis CR450x3). A custom-written MATLAB routine was used to extract the evaporation rate and contact angles of the droplets [7].

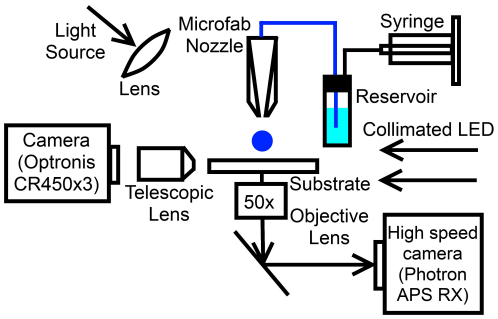

Figure 1. *Schematic of the imaging set-up used for visualizing internal flows and side profiles of picolitre droplets.*

MATLAB code based on routines developed at Georgetown University [8] were used for the particle tracking. The drying time, t_{dry}, was defined as the time when the volume reached zero.

Higher volume fractions of polystyrene spheres (1%w and 5%w) were included in the laponite suspensions to determine the deposit structure. Dried deposits were sputter-coated with gold (five coats at 1.2 kV, 35 mA for 30 s) before imaging with a scanning electron microscope (SEM, Philips XL30 Environmental SEM). A white light interferometer (Zygo NiewView 5000) provided vertical profiles of the dried deposits.

Rheological data were collected at 293 K using an AR 2000 Rheometer (TA Instruments) with a cone (2° angle) and plate geometry for laponite suspensions without the inclusion of polystyrene spheres. The steady-state viscosity of each fluid was recorded over a range of shear rates (0.1–1500 s^{-1}). Recovery times were investigated by applying a stepped shear rate with fast sampling.

Surface tension measurements for each component were obtained using a pendant drop tensiometer (First Ten Angstroms, FTA200).

Results and Discussion

Laponite suspensions shear-thin at laponite concentrations above $\backsim$2.5%w (Figure 2). The networked structure of the laponite breaks down at the high shear rates inside an inkjet printhead ($10^4\,\mathrm{s}^{-1}$). Once on the substrate (at low shear $\backsim 1\,\mathrm{s}^{-1}$), the network reforms, increasing the viscosity and elasticity (for gels). A sol−gel transition occurs between 2.8−3%w laponite (determined by inverted bottle experiments and confirmed with rheology measurements). Once the laponite concentration is sufficient to form a gel, the suspension has a finite yield stress (Table 1). At higher laponite concentrations the yield stress of the gel increases.

To utilise the sol−gel transition as a method for reducing ring stain formation in drying droplets, the speed at which the

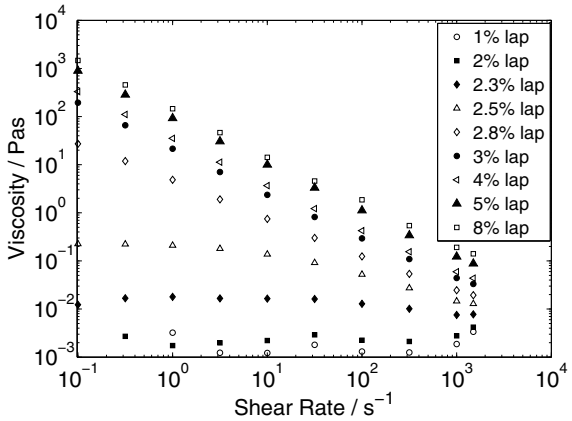

Figure 2. *The shear viscosity of laponite suspensions at various shear rates. Suspensions are shear-thinning above 2.5%w laponite.*

Table 1: Yield stresses determined by oscillatory measurements for laponite suspensions in water at various laponite concentrations.

Laponite concentration / %w	Yield stress / Pa
2.8	0.3
3.0	5
4.0	45
5.0	107
8.0	149

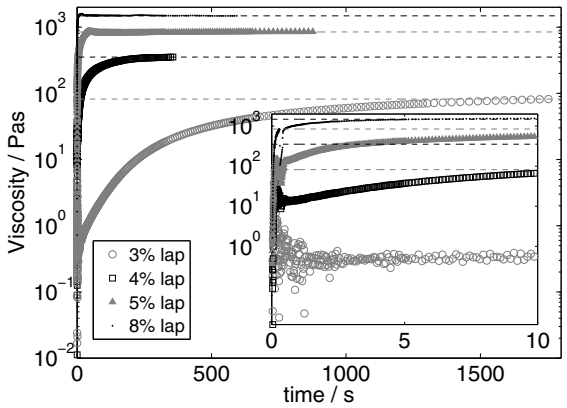

Figure 3. *Recovery of the shear viscosity of laponite suspensions. Dashed lines indicate full recovery.*

laponite network recovers following break-up in the inkjet nozzle must be on a timescale that is fast compared to the droplet drying time. Figure 3 indicates that an 8%w laponite suspension can fully recover within the drying lifetime of a droplet ($\backsim$4 s). Rheological data indicates that higher laponite concentrations recovered the networked-structure faster than low laponite concentrations. The fast recovery of the network was also confirmed by the capability to undergo a sol-gel transition during droplet drying. For the elasticity of the laponite suspension to be sufficient to prevent particle motion, the concentration of laponite

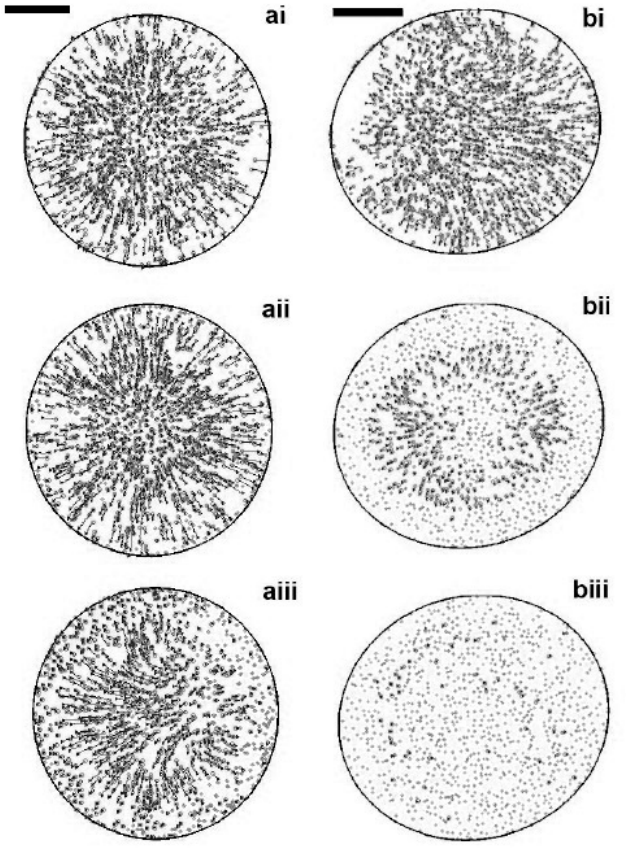

Figure 4. *Particle tracks for droplets of a) pure water (t_{dry}=5.03 s) and b) 2%w laponite (t_{dry}=6.32 s) for i) 0-0.1t_{dry}, ii) 0.4-0.5t_{dry} and iii) 0.7-0.8t_{dry}, where t_{dry} is the drying time of the droplet. Stationary particles are in light gray and moving particles in black. Scale bars are 50 μm.*

during drying is essential to ensure a high enough yield stress to overcome capillary flow and a fast recovery time (of the network) on the timescale of drying.

Adding tracer particles to the laponite suspensions enabled the visualisation of internal flows within drying inkjet-sized droplets. Ring stains formed in water droplets drying with a pinned contact line, due to radial flow towards the periphery (Figure 4a). De-pinning of the contact line in the late stages of drying dragged particles to the left of the droplet (Fig. 4aiii).

In droplets of laponite suspensions, the clay concentration increased throughout drying as solvent was lost from the droplet. For a sessile droplet, the evaporative flux is not uniform along the liquid-vapor interface, and enhanced evaporation at the contact line caused further concentration of laponite in this region. For the droplet with an initial laponite concentration of 2%w, further evaporation-driven concentration of the laponite to 2.8−3%w induced a sol-gel transition at low shear rates. The gelling front traveled from the contact line inward, fixing particle positions in the gel (Figure 4bii). Hence, an initial laponite concentration of 2%w was sufficient to allow particle positions to be "fixed" in the deposit. Additionally, the laponite pinned the contact line, ensur-

ing a well-defined edge to the deposit.

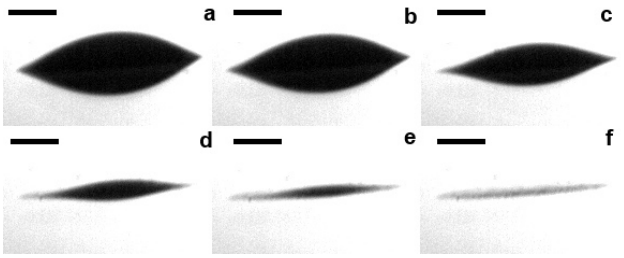

Figure 5. *The side profile of a water droplet containing 3%w laponite and 0.05%w 1-μm polystyrene spheres after fractions of a) 0.1, b) 0.2, c) 0.5, d) 0.8, e) 0.9 and f) 1.0 of the drying time, t_{dry}. The drying time was 8.64 s. Scale bars are 50 μm.*

Table 2: Surface tension values, σ, for each component in water at 20°C.

Component	Water	1%w laponite	2%w laponite
σ / mNm^{-1}	72.5	70.4	69.9

For a droplet containing an initial laponite concentration of 3%w, there was a small amount of radial flow during the first stages of drying as the networked structure recovered post-jetting. Following recovery, particles were stationary in the gel.

Side profiles of the droplets revealed that at laponite concentrations of 2%w and 3%w, the droplet shape deviated from a spherical cap. Instead, a sol "cap" and gel "disk" formed (see Fig. 5). With the gel extending inwards as solvent evaporated from the droplet. This provides evidence that the laponite elasticity was sufficient to deform the droplet from a spherical cap, i.e. the yield stress is sufficient to overcome the capillary pressure.

In some cases, the addition of nanoparticles to a fluid can cause changes to the surface tension. As a lower contact angle can cause a decreased capillary pressure (reducing capillary flow) within a drying droplet, we confirmed that the surface tension of the laponite suspensions did not differ significantly from that of water (Table 2). The small differences in surface tension let us conclude that the influence of laponite on the capillary pressure (and on the elastic modulus required to prevent particle motion) is small.

The effect of laponite on the deposit was observed by increasing the concentration of polystyrene spheres loaded in the droplets. Scanning electron micrographs reveal the particle distributions formed from droplets containing 1%w polystyrene spheres (Figure 6) and 5%w polystyrene spheres (Figure 7). Vertical profiles, examined using interferometry, are given in Figure 8 and Figure 9.

At a polystyrene sphere concentration of 1%w, the deposit from a water droplet gave non-uniform coverage. Conversely, laponite concentrations of 2.5%w and 2.8%w produced a fairly uniform height distribution across the droplet (see Fig. 8). When the laponite concentration was lowered to 2%w, a significant decrease in height was observed at the center of the deposit compared to the contact line.

Deposits containing 5%w polystyrene spheres gave a ring stain when no laponite was included (Figure 7a). The ring is confirmed by vertical profiles of the deposits (Figure 9). Complete

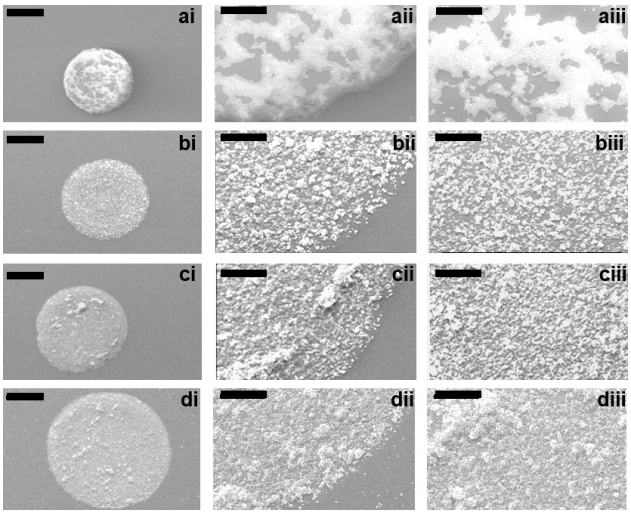

Figure 6. *Scanning electron micrographs of deposits on as-received glass from droplets containing 1%w 200 nm polystyrene spheres and a) water, b) 2.8%w laponite, c) 2.5%w laponite, d) 2.0%w laponite. The whole deposit (i) and zooms to the contact line (ii) and interior (iii) are given. Scale bars are 50 μm for the whole deposit and 10 μm for the zooms.*

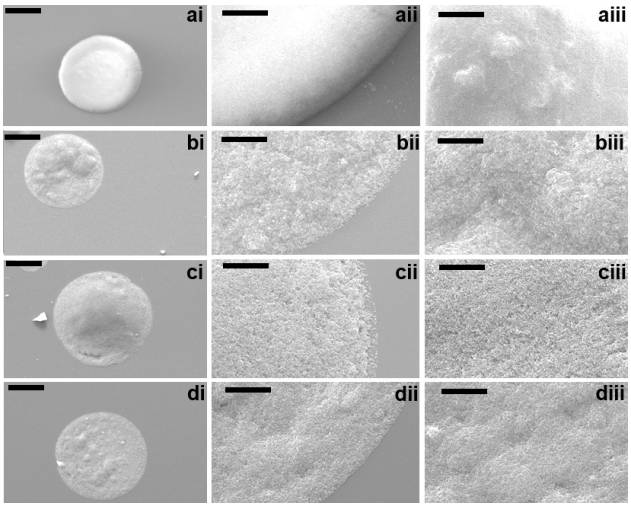

Figure 7. *Scanning electron micrographs of deposits on as-received glass from droplets containing 5%w 200 nm polystyrene spheres and a) water, b) 2%w laponite, c) 1%w laponite, d) 0.8%w laponite. The whole deposit (i) and zooms to the contact line (ii) and interior (iii) are given. Scale bars are 50 μm for the whole deposit and 10 μm for the zooms.*

prevention of radial flow at high laponite concentrations formed a domed deposit. In order to form a uniform deposit, a controlled amount of radial flow was required, limited by the sol-gel transition. On forming a gel, the elastic modulus of the suspension was sufficient to overcome the capillary flow, preventing further particle motion. Figures 7 and 9 indicate that at a polystyrene sphere concentration of 5%w, 0.8%w laponite was sufficient to form a uniform deposit. Laponite concentrations of $\geq$1%w produced a dome (with 5%w polystyrene spheres). At this higher concentration of polystyrene spheres, a lower laponite concentration was required to achieve a uniform deposit.

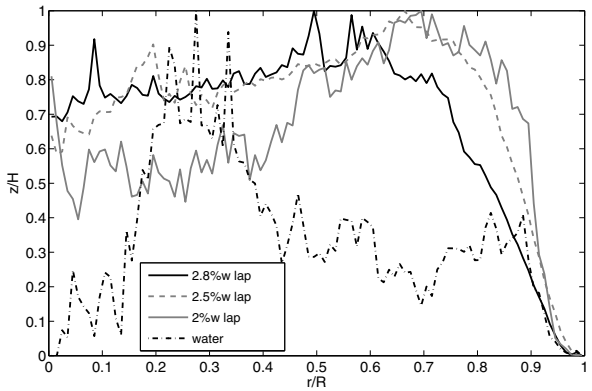

Figure 8. *Distribution of the deposit height, z, with radial co-ordinate, r, for various laponite suspensions containing 1%w 200 nm polystyrene spheres. The radial co-ordinate is normalized by the deposit contact radius, R. The deposit height, z, is normalised by the maximum height of the deposit, H.*

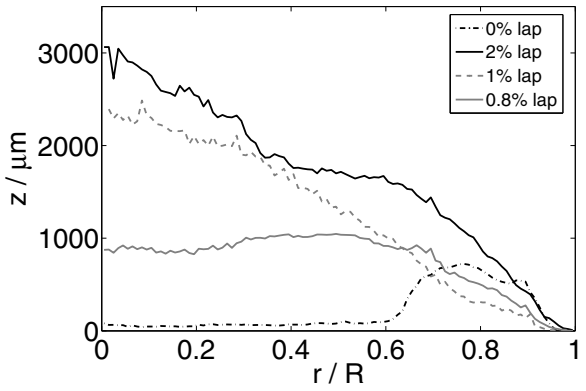

Figure 9. *Distribution of the deposit height, z, with radial co-ordinate, r, for various laponite suspensions containing 5%w 200 nm polystyrene spheres. The radial co-ordinate is normalized by the deposit contact radius, R.*

Conclusion

The sol−gel transition in laponite suspensions can be used to control the distribution of particulates within the suspension. As the laponite concentrates during drying, the transition from a sol to a gel increases the elasticity (and yield stress) of the suspension. When the yield stress is large enough to overcome the capillary pressure, then particle motion ceases. Due to non-uniform evaporation, the droplet gels from the contact line inwards. By controlling the laponite concentration, and hence the timing of the gelling, we can dictate the amount of radial flow required to generate a uniform deposit: too little radial flow and a domed structure forms, too much and a ring stain is produced.

The finite time taken to rebuild the laponite network is also important: if the network rebuilds too quickly, the droplet will gel before radial flow begins and a domed deposit will form; if it is too slow the droplet will gel too late in the drying process, giving a ring stain. The network recovers faster as the laponite concentration increases, and it is the balance of the increasing concentration of laponite during drying and the corresponding decrease in the recovery time that provides the necessary control over the gelling of the droplet.

The final deposit includes laponite, which may not be desirable for some applications. Alternative gelling agents could be used, provided that an evaporation-driven gelling transition occurs on a timescale that is short compared to the drying lifetime of the droplet.

Acknowledgments

The authors thank S. Biggs and H.N. Yow (University of Leeds, UK) for the polystyrene spheres. This work was financed by EPSRC (grant EP/H018913/1).

References

[1] R.D. Deegan, O. Bakajin, T.F. Dupont, G. Huber, S.R. Nagel and T.A. Witten, Nature **389**, 6653, 827–829 (1997).

[2] R.D. Deegan, O. Bakajin, T.F. Dupont, G. Huber, S.R. Nagel and T.A. Witten, Phys. Rev. E **62**, 1, 756–765 (2000).

[3] X. Shen, C.-M. Ho and T.-S.Wong, J. Phys. Chem. B **114**, 16, 5269–5274, (2010).

[4] R. Dou, T. Wang, Y. Guo and B. Derby, J. Am. Ceram. Soc. **94**, 11, 3787-3792, (2011).

[5] A. Friederich, J.R. Binder and W. Bauer, J. Am. Ceram. Soc. **1**, 7, 1–7, (2013).

[6] E. L. Talbot, L. Yang, A. Berson and C. D. Bain, Appl. Mater. Interf., accepted, DOI: 10.1021/am501966n.

[7] E.L. Talbot, A. Berson, P.S. Brown and C.D. Bain, Phys. Rev. E **85**, 061604, (2012).

[8] `http://physics.georgetown.edu/matlab/tutorial.html`. Viewed 15/7/13.

Author Biography

Emma Talbot received her MSci Joint Honors in Chemistry and Physics from the University of Durham, UK in 2010. She remained at the University of Durham for her PhD (supervised by C.D. Bain) and submitted her doctoral thesis in April 2014 titled "Drying Inkjet Droplets: Internal Flows and Deposit Structure".